SOLAR RADIATION AT THE EARTH'S SURFACE: ITS CALCULATION AND INFERENCE FROM SATELLITE IMAGERY

Fred L. Bartman
University of Michigan
Ann Arbor, Michigan

INTRODUCTION: PHYSICAL AND EMPIRICAL MODELS

Solar radiation incident at the surface has not been measured at all locations on the Earth's surface. A valuable supplement to measured values are calculated values. This paper discusses a few methods for calculation of the insolation on a horizontal surface and refers to some of the many papers in the literature dealing with this topic.

A valuable reference for this paper has been the notes for the intensive short course entitled "Solar Energy Measurements and Instrumentation" which was presented as part of the University of Michigan Engineering Summer Conference Program on July 9-10, 1979. The notes were written by staff members in the Department of Atmospheric and Oceanic Science. Of particularly great help in the preparation of this paper is Chapter 8 of those notes, "Modelling of Received Solar Radiation," by W. R. Kuhn.

The various calculations can be broadly grouped into two categories, physical models and empirical models. Physical models use the basic physical principles of radiative transfer. They require the input of those quantities involved in the attenuation of the solar beam as it passes through the atmosphere. Data on these factors, i.e., the vertical distribution of water vapor and ozone, the aerosol vertical distribution, particle size distribution, and index of refraction, the physical characteristics of clouds, and the reflectivity of the Earth's surface, are not always available and are highly variable. In addition, the calculations are quite elaborate. Thus the other type of model, the empirical one, is often desirable. Empirical models are generally developed by using a known data set to calculate a set of regression coefficients for some set of parameters, such as the solar zenith angle, the duration of sunshine, or the amount of opaque cloud cover. Then the model can be used to predict the incident solar radiation for other values of the parameters. These models are easy to use but must be applied with care.

The advent of satellite remote sensing of clouds and the surface make the use of empirical models employing satellite images possible. Such a technique is also discussed.

In all the following sections, the surface receiving solar radiation is assumed to be horizontal. The case of solar radiation incident on an inclined plane is not discussed here.

PHYSICAL MODELS

Under clear sky conditions, we can write an equation for the flux (F) of radiation arriving at the surface as

$$F = I \cos \theta + D \tag{1}$$

where F is the global solar radiation (W/m^2), I is the direct beam of solar radiation, D is the diffuse component, and θ is the solar zenith angle.

Spectral Calculations

In terms of spectral components, I and D above can be written as

$$I = \int_0^\infty I_\lambda(0) \exp(-\tau_\lambda \sec \theta)\, d\lambda \tag{2a}$$

$$D = \int_0^\infty D_\lambda\, d\lambda \tag{2b}$$

where $I_\lambda(0)$ is the spectral solar irradiance at the top of the atmosphere, τ_λ is the spectral extinction optical depth, and λ is wavelength (μm).

The extinction is due primarily to absorption by ozone (O_3) and water vapor (H_2O), to scattering by air molecules, i.e., Rayleigh scattering (R), and to absorption and scattering by aerosols (A). Thus,

$$\tau_\lambda = \tau_\lambda(R) + \tau_\lambda(O_3) + \tau_\lambda(H_2O) + \tau_\lambda(A) \tag{3}$$

Leckner (1978) presented expressions for these extinction coefficients. The Rayleigh scattering extinction coefficient is given by

$$\tau_\lambda(R) = 0.008735\lambda^{-4.08} \frac{p}{p_o} \tag{4}$$

where p is the surface pressure (mbar) and p_o is 1013 mbar. For ozone,

$$\tau_\lambda(O_3) = -k(\lambda)\, \ell \tag{5}$$

where $k(\lambda)$ are spectral absorption coefficients (cm^{-1}) given in table I and ℓ is the total ozone amount in atm cm.

The optical depth for water vapor can be written as (see also McClatchey et al., 1971)

$$\tau_\lambda(H_2O) = \frac{0.3\ k_w(\lambda)\ X_w}{\left[1 + 25.35\ k_w(\lambda)\ X_w m\right]^{0.45}} \tag{6}$$

where $k_w(\lambda)$ are effective absorption coefficients of water vapor (cm^2-g^{-1}), X_w is the total precipitable water (g/cm^2), and $m = \sec\theta$, the optical air mass. The values of $k_w(\lambda)$ are given in table II.

The aerosol optical depth can be quite accurately written as

$$\tau_\lambda(A) = \int_0^\infty n(z)\ Q_\lambda(z)\ \pi[r(z)]^2\ dz \tag{7}$$

where $n(z)$ is the aerosol number density at height z, $Q_\lambda(z)$ is the mean spectral extinction efficiency for the aerosols at altitude z, and $r(z)$ is the mean aerosol radius at altitude z. Since the vertical variations of aerosol concentration, composition, size distribution, and index of refraction are difficult to know, it is best to use the simple power law expression for aerosol attenuation

$$\tau_\lambda(A) = -\beta\lambda^{-\alpha} \tag{8}$$

where β is the turbidity coefficient and α is the wavelength coefficient.

Measurements of α indicate a wide range of possible values. However, most values occur in the range from 0.8 to 2, with an average value of 1.3 being considered most reasonable. The turbidity coefficient can be measured with reasonable accuracy. Typical values are shown in table III.

The spectral diffuse component of solar radiation can be written as

$$D_\lambda = 0.5\left(I_\lambda(0)\ \exp\left\{-\left[\tau_\lambda(O_3) + \tau_\lambda(H_2O)\right] m\right\} - I_\lambda\right) \cos\theta \tag{9}$$

Leckner (1978) has made calculations of this kind and compared them with experimental measurements in a case where β was known to lie in the range from 0.05 to 0.1. The results are shown in figures 1 and 2.

Calculations for the Total Integrated Solar Radiation

The previous section indicates that the spectral calculation for solar radiation at the surface is fairly complex. Some simplification is achieved

when the integrated values are calculated with wavelength-averaged values of the parameters involved and with aerosol effects neglected.

An effective mean value of Rayleigh optical depth $\bar{\tau}_\theta(R)$ is given in table IV as a function of zenith angle. The tabulated values refer to a vertical path only. Thus the direct solar radiation reaching the surface if the only extinction process were Rayleigh scattering would be

$$F(R) = I_0 \cos\theta \exp\left[-\bar{\tau}_\theta(R) \frac{p}{1013} \sec\theta\right] \tag{10}$$

where I_0 is the solar constant, θ is the zenith angle, and p is the surface pressure in mbar. The values of table IV can be calculated from

$$\bar{\tau}_\theta(R) = \frac{1}{\sec\theta} \ln\left\{\frac{\int_0^\infty I_\lambda(0)\, d\lambda}{\int_0^\infty I_\lambda(0) \exp\left[-\tau_\lambda(R) \sec\theta\right] d\lambda}\right\} \tag{11}$$

For ozone, the effective absorptance $\alpha(O_3)$ over the entire solar spectrum is given by Lacis and Hansen (1974) as

$$\alpha(O_3) = \frac{0.02118u}{1 + 0.042u + 3.23 \times 10^{-4} u^2} + \frac{1.082u}{(1 + 138.6u)^{0.805}} + \frac{0.0658u}{1 + (103.6u)^3} \tag{12}$$

where

$$u = \ell \sec\theta \tag{13}$$

The effective absorptance for water vapor according to Lacis and Hansen (1974) is

$$\alpha(H_2O) = \frac{2.9w}{(1 + 141.5w)^{0.635} + 5.925w} \tag{14}$$

where

$$w = X_w \cos\theta \tag{15}$$

Ozone absorption and Rayleigh scattering occur in the same region of the spectrum, but ozone absorption is at high altitudes where there is little Rayleigh scattering. Therefore the solar radiation reaching the surface if there were only attenuation by ozone and Rayleigh scattering would be

$$F(R,H_2O) = I_0 \cos\theta \exp\left[-\bar{\tau}_\theta(R) \frac{p}{1013} \sec\theta\right] [1 - \alpha(O_3)] \tag{16}$$

Water vapor absorption occurs in the near-infrared region of the spectrum where ozone absorption and Rayleigh scattering are negligible. Thus the attenuation by water vapor can be subtracted directly from equation (16) to yield the direct solar beam of radiation at the surface as

$$I = I_0 \cos\theta \left\{ \exp\left[-\bar{\tau}_\theta(R) \frac{p}{1013} \sec\theta\right] [1 - \alpha(O_3)] - \alpha(H_2O) \right\} \tag{17}$$

The diffuse radiation arriving at the surface consists of the solar radiation scattered downward by the molecules and aerosols. With scattering by aerosols neglected, scattering downward to the surface can be approximated by the following equation (Paltridge and Platt, 1976):

$$D = \left[(I_0 - I) \cos\theta - I_0 \cos\theta \, \alpha_R(\theta)\right] \left(1 + \alpha_g \bar{\alpha}_R^*\right) + I \cos\theta \, \alpha_g \alpha_R^* \tag{18}$$

In equation (18), $(I_0 - I)$ is the radiation removed from the direct beam by scattering, $I_0 \cos\theta \, \alpha_R(\theta)$ is the upward scattered radiation, and $\alpha_R(\theta)$ is an approximate coefficient for upward scattering (i.e. atmospheric reflection) given by Lacis and Hansen (1974) as

$$\alpha_R(\theta) = \frac{0.28}{1 + 6.43 \cos\theta} \tag{19}$$

The term $\alpha_g \bar{\alpha}_R^*$ takes into account the downward scattering of the diffuse radiation reflected from the surface; α_g is the ground albedo, and $\bar{\alpha}_R^*$ the reflection coefficient for downward scattering, about 0.0685. The last term in equation (18) is the direct beam radiation which is reflected from the Earth and then scattered back downward.

EMPIRICAL MODELS

Clear Sky: Zenith Angle Variation

Under clear sky conditions, zenith angle is the main factor affecting the solar radiation arriving at the surface at a given location. In this case empirical relations can represent the long time average of direct, diffuse, and global solar radiation with good accuracy. For example, Paltridge and Platt (1976) derived empirical functions from data taken at Aspendale, Victoria, Australia, for the 5-year period from 1967 to 1972. The data and empirical curves are shown in figures 3 to 5. The empirical functions are as follows.

For global solar radiation on a horizontal surface, at Aspendale (latitude $38^{\circ}02'S$), the hourly total ($mW\text{-}hr/cm^2$) is

$$F = 1.0 + 141.1 \sin \gamma - 31.0 (\sin \gamma)^{1/2} \tag{20}$$

where γ is the solar elevation angle. The direct normal solar radiation is given by

$$I = 100.0[1 - \exp(-0.06\gamma)] \tag{21}$$

and the diffuse radiation on a horizontal plane by

$$D = 0.5 + 9.6[1 - \exp(-0.05\gamma)] \tag{22}$$

Cloudy Skies

It is difficult to treat clouds in solar energy calculations. Detailed studies require knowledge of cloud drop size distribution and cloud total water content. Although clouds generally diminish the solar radiation incident on the surface, the surface radiation may actually be increased under partially cloudy conditions if the solar disk is not occulted.

Table V indicates the percent decrease in flux of total surface radiation due to continuous cloud cover of various types as a function of the solar zenith angle (Kondrat'ev, 1973).

An empirical expression that yields reasonably accurate results for mean annual and mean monthly studies is (Berliand, 1961) for global radiation:

$$F = F_0(1 - an - bn^2) \tag{23}$$

where F_0 is the clear sky radiation, $b = 0.38$, a is a coefficient that varies with latitude as shown in table VI, and n is cloud cover in tenths. This relation should be used only for long time averages and not for calculations on a daily basis.

Models of the Air Resources Laboratory (NOAA)

The Air Resources Laboratory of NOAA has developed empirical models of global solar radiation on a horizontal plane. The models were developed for the rehabilitation of historical data archives for 26 stations in the NOAA solar radiation network (Solmet, 1978). The data tapes consisted of hourly records of observed weather data and

1. Integrated hourly global solar radiation
2. Duration of sunshine in minutes
3. Cloud opacity in tenths
4. Cloud cover in tenths
5. Sky condition observations

Five regression equations were developed and used for those stations with an appropriate data set for the regression analysis. The form of the equations for each model and examples of the parameters are as follows:

1. Clear Sky

$$SRC = A_0 + A_1 \cos(ZA) + A_2 \cos^2(ZA) + A_3 \cos^3(ZA) \quad (24)$$

where SRC is the clear sky hourly integral global solar radiation (kJ/m^2) and ZA is zenith angle. The coefficient A_0 is determined for mornings and afternoons for each month of the year; and A_1, A_2, and A_3 are estimated separately for mornings and afternoons, one set of each for the year.

2. Sunshine and Opaque Cloud (preferred estimating function)

$$SR = SRC\left[B_0 + B_1(SS) + B_2(OPQ) + B_3(OPQ)^2 + B_4(OPQ)^3 + B_5(RN)\right] \quad (25)$$

where SR is the hourly global solar radiation (kJ/m^2), SS is the number of minutes of sunshine divided by 60, OPQ is cloud opacity (0.1, 0.2, etc.), and RN is a precipitation variable which is 0 for no precipitation and 1 when precipitation is reported.

3. Opaque Cloud Only (same as 2 without sunshine term)

$$SR = SRC\left[C_0 + C_2(OPQ) + C_3(OPQ)^2 + C_4(OPQ)^3 + C_5(RN)\right] \quad (26)$$

4. Sunshine Only (converse of 3)

$$SR = SRC[D_0 + D_1(SS) + D_5(RN)] \quad (27)$$

5. Sky Condition

$$SR = SRC\left[E_0 + \sum_{j=1}^{7} E_i(SC_i) + E_8(RN)\right] \quad (28)$$

where each SC_i is 0 or 1 depending on whether the sky cover listed below is present at any one of up to four levels:

SC_1 thin scattered; 0.1-0.5 cover

SC_2 opaque scattered; 0.1-0.5 cover

SC_3 thin broken; 0.6-0.9 cover

SC_4 opaque broken; 0.6-0.9 cover

SC_5 thin overcast; 1.0 cover

SC_6 opaque overcast; 1.0 cover

SC_7 partial or total obscuration

The coefficients for the regression equations are available on punched cards; an example is listed below. The punched cards are arranged to provide a maximum of 12 fields of length 6 (including the decimal point). The last 8 columns of each card are identification. There are 7 cards for each station as follows:

Card order	Parameter	Number of coefficients	Number of punched fields on card	Description
1	A_0	12	12	Clear sky; Jan-Dec, morning
2	A_0	12	12	Clear sky; Jan-Dec, afternoon
3	A_1, A_2, A_3	6	6	Clear sky; first 3 are morning; last 3 are afternoon
*4	$C_0 - C_5$	5	6	Opaque cloud only: SS coef. = 0.0 ($C_1 = 0$)
*5	$B_0 - B_5$	6	6	Sunshine and opaque cloud coef.
*6	$D_0 - D_5$	3	6	Sunshine only: opaque cloud coefs. = 0.0 ($d_2 = d_3 = d_4 = 0$)
7	$E_0 - E_8$	9	9	Sky cond. coef.

*Cards 4, 5, and 6 have common ordered positions for the constant term, SS, OPQ, OPQ^2, OPQ^3, and RN. For example, on card 4 the sunshine coefficient (field 2) is always zero.

An example of a set of coefficients is

Washington, D.C.

```
-5.   12.   1.    -30.  -89.  -180. -219. -192. -128. -65.  -37.  -26.  WSH CLRM
9.    9.    20.   -30.  -87.  -172. -176. -195. -131. -67.  -59.  -15.  WSH CLRA
2350. 2810. -1540. 2100. 3570. -2060.                                   WSH CLRZ
1.000 0.000 -.474 0.920 1.070 -.214                                     WSH 0
0.000 0.000 0.000 0.000 0.000 0.000                                     WSH SS.0
0.000 0.000 0.000 0.000 0.000 0.000                                     WSH SS
0.932 0.048 -.005 -.007 -.141 -.055 -.471 -.131 -.251                   WSH SKYC
```

THE INFERENCE OF SOLAR RADIATION AT THE SURFACE FROM SATELLITE DATA

The technique involved in the application of satellite images to the prediction of solar radiation arriving at the Earth's surface has three steps:

1. Establish a set of equations which can be used to relate the data from the satellite images to the insolation. It may also be necessary to include some conventional meteorological parameters in the equations.

2. Use satellite data for a period of time plus surface solar energy measurements taken at the same time to determine unknown constants in these equations.

3. Then use satellite image data with the equations to predict the solar radiation incident upon the surface.

In the following, one of the more recent attempts, estimating hourly and daily global solar radiation from GOES geostationary satellite images, is discussed.

The Great Plains Experiment

The National Environmental Satellite Service and the Great Plains Agricultural Council have carried out an experiment to determine incoming solar radiation in the U.S. Great Plains area from geostationary satellite images (Tarpley, 1979).

The region selected for the experiment, shown in figure 6, was bounded by two latitude circles, 29° and 49° N, and two meridians of longitude, 95° and 105° W. Twenty-two sites were instrumented with pyranometers for measurement of incident global surface energy at the points shown in the figure.

The satellite data used were visible (0.55 to 0.75 μm) images from the GOES visible and infrared spin scan radiometer (VISSR), having 8 km resolution at Nadir. Relative brightness levels were digitized (0 to 63 counts). Hourly images were used for 7 to 10 hours per day distributed about local noon for the period from June 7, 1977, to August 15, 1977.

Surface meteorological data used were surface pressures and total precipitable water.

The grid used for analyses of the satellite images is shown in figure 7. The Great Plains area was divided into targets approximately 50 km on a side, each made up of 7 × 6 arrays of 8 km pixels.

Quantities used as variables for determination of surface insolation were

1. Surface pressure, a measure of total air mass, which therefore should be correlated with the depletion of solar radiation by molecular scattering

2. Precipitable water which provides information on absorption and scattering by water vapor

3. Mean target brightness which is a measure of reflected and scattered radiation due to all causes

4. Cloud amount and brightness which indicate the amount of radiation reflected by the clouds.

Determination of Cloud Free Brightness Levels

An initial task was to determine cloud free brightness in the images, by regression against functions of solar zenith angle χ and the azimuth angle ϕ between the Sun and the satellite. Cloud free brightness was calculated on a 2^{o} grid with interpolation to determine values at 0.5^{o} target intervals. For this purpose, 100 observations per target were used for 27 days in May 1977, just previous to the period of the test.

In order to obtain the regression coefficients, cloud contaminated observations were eliminated by an automatic cloud detection and elimination procedure, along with fitting the data to the cloud free regression equation of the form

$$B = A + b \cos \chi + c \sin \chi \cos \phi + d \sin \chi \cos^{2}\phi \tag{29}$$

The cyclic procedure, shown in figure 8, produced cloud free data sets and regression coefficients after two iterations of the procedure, with the final standard error of the estimate for the regression equation of 0.5 to 0.9 counts.

Determination of Cloud Parameters and Target Brightness

The cloudiness of each pixel was established according to the following criteria: it was clear if the brightness was less than or equal to $B(\chi,\phi) + 3$, partly cloudy if the brightness was greater than $B(\chi,\phi) + 3$ but less than or equal to $B(\chi,\phi) + 5$, and cloudy if the brightness was greater than $B(\chi,\phi) + 5$.

The cloud fraction for the target was then calculated from

$$n = \frac{0.5N_2 + N_3}{N_1 + N_2 + N_3} \tag{30}$$

where N_1, N_2, and N_3 were the number of pixels in the clear, partly cloudy, and cloudy cases.

The mean cloud brightness I_{cld} was taken to be the mean of the brightness for the cloudy cases. The quantity

$$B_0 = B(45^o, 105^o) \tag{31}$$

was also calculated as the normalized clear brightness.

Estimation of Hourly Insolation

The form of the regression equations for hourly insolation was suggested by consideration of the equation of conservation of radiant energy

$$Q_0 = Q_R + Q_A + Q_G \tag{32}$$

where the subscripts indicate the following:

0	at the top of the atmosphere
R	reflected back into space
A	absorbed in the atmosphere
G	absorbed at the ground

But

$$Q_G = Q_S(1 - \alpha) \tag{33}$$

where Q_S is the insolation at the surface and α is the surface albedo. Substituting from equation (32) for Q_G results in

$$Q_S = \frac{1}{1 - \alpha}(Q_0 - Q_R - Q_A) \tag{34}$$

The regression equations used were determined by cloud amount; they were

$$\left.\begin{aligned} Q_S &= a + b\cos\chi + c\psi + dn + e\left(\frac{I_m}{B}\right)^2 && (n < 0.4) \\ Q_S &= a + b\cos\chi + cn\left(\frac{I_{cld}}{B_0}\right)^2 && (0.4 \leq n < 1.0) \\ Q_S &= a + b\cos\chi + c\left(\frac{I_{cld}}{B_0}\right) && (n = 1.0) \end{aligned}\right\} \tag{35}$$

where

Q_S	hourly surface insolation, ly (1 langley = 41.84 kJ/m^2)
χ	local solar zenith angle
ψ	transmittance of the clear atmosphere
n	fractional cloud amount
I_m	mean target brightness
I_{cld}	mean cloud brightness
B	predicted clear brightness
B_0	normalized clear brightness, $B(45^o,105^o)$
a,b,c,d,e	the regression coefficients

Precipitable water and surface altitude Z were used in the determination of the clear target transmission:

$$\psi = \psi_{ws}\psi_{wa}\psi_r \tag{36}$$

where the transmission due to water vapor scattering, water vapor absorption, and Rayleigh scattering, respectively, were taken to be:

$$\psi_{ws} = 1 - 0.00225wm \tag{37}$$

$$\psi_{wa} = 1 - 0.077(wm)^{0.3} \tag{38}$$

$$\psi_r = 0.972 - 0.0862m + 0.00933m^2 \tag{39}$$

where w is the precipitable water and m, the optical air mass, is given by

$$m = \sec \chi \exp\left(-\frac{Z}{8243}\right) \tag{40}$$

Results

To determine the technique for estimating surface insolation from cloud images, all of the data were included. This is referred to as the dependent development data set. In order to estimate how accurately insolation could be estimated under operational conditions, the data were divided into two parts, the dependent set with only 4 pyranometer sites and the independent set with 18 pyranometers to verify the regression equation.

The values of the regression coefficients and their standard errors are listed in table VII for the dependent developmental data set. For this set, satellite estimates from the regression equations are plotted versus actual measurements in figures 9(a), 9(b), and 9(c) for $n < 0.4$, $0.4 \leq n < 1.0$, and $n = 1.0$, respectively. Correlation coefficients and standard errors of the estimates are shown in the figures.

Daily cumulative insolation was also estimated, using the zenith angle to interpolate and fill in gaps in the data. These results are shown in figure 10.

Finally the statistics of estimated total insolation for four different cases are shown in table VIII. Cases considered are

1. Seven or more pictures per day, dependent data

2. Seven or more pictures per day, independent data

3. Two pictures per day, dependent data

4. One picture per day, dependent data

In each of the first three cases, the standard errors are less than 10 percent of the mean. In the last case, with only one picture per day, the standard error was about 20 percent of the mean. In this last case, sampling was insufficient.

The most significant problem with the technique is the overestimation of surface insolation under cloudy conditions (see fig. 9(c)).

REFERENCES

Berliand, T. G. 1961: Distribution of Solar Radiation Over the Continents. Gidrometdoiydat (Leningrad).

Kondrat'ev, K. Ya., ed. 1973: Radiation Characteristics of the Atmosphere and the Earth's Surface. NASA TT F-678, Amerind Pub. Co. Pvt. Ltd. (Available from NTIS.)

Lacis, Andrew A.; and Hansen, James E. 1974: A Parametrization for the Absorption of Solar Radiation in the Earth's Atmosphere. J. Atmos. Sci., vol. 31, no. 1, pp. 118-133.

Leckner, Bo 1978: The Spectral Distribution of Solar Radiation at the Earth's Surface - Elements of a Model. Sol. Energy, vol. 20, no. 2, pp. 143-150.

McClatchey, R. A.; Fenn, R. W.; Selby, J. E. A.; Volz, F. E.; and Garing, J. S. 1971: Optical Properties of the Atmosphere (Revised). AFCRL-71-0279, U.S. Air Force. (Available from DTIC as AD 726 116.)

Paltridge, G. W.; and Platt, G. M. R. 1976: Radiative Processes in Meteorology and Climatology. Elsevier Scientific Pub. Co.

Solmet, 1978: Solmet Manual - Volume 2. National Climatic Center.

Tarpley, J. D. 1979: Estimating Incident Solar Radiation at the Surface From Geostationary Satellite Data. J. Appl. Meteorol., vol. 18, no. 9, pp. 1172-1181.

TABLE I.- SPECTRAL ABSORPTION COEFFICIENTS OF OZONE (cm^{-1})

[From Leckner, 1978*]

λ	k	λ	k	λ	k	λ	k	λ	k
0.290	38.000	0.445	0.003	0.515	0.045	0.585	0.118	0.700	0.023
0.295	20.000	0.450	0.003	0.520	0.048	0.590	0.115	0.710	0.018
0.300	10.000	0.455	0.004	0.525	0.057	0.595	0.120	0.720	0.014
0.305	4.800	0.460	0.006	0.530	0.063	0.600	0.125	0.730	0.011
0.310	2.700	0.465	0.008	0.535	0.070	0.605	0.130	0.740	0.010
0.315	1.350	0.470	0.009	0.540	0.075	0.610	0.120	0.750	0.009
0.320	0.800	0.475	0.012	0.545	0.080	0.620	0.105	0.760	0.007
0.325	0.380	0.480	0.014	0.550	0.085	0.630	0.090	0.770	0.004
0.330	0.160	0.485	0.017	0.555	0.095	0.640	0.079	0.780	0.0
0.335	0.075	0.490	0.021	0.560	0.103	0.650	0.067	0.790	0.0
0.340	0.040	0.495	0.025	0.565	0.110	0.660	0.057	0.800	0.0
0.345	0.019	0.500	0.030	0.570	0.120	0.670	0.048	0.810	0.0
0.350	0.007	0.505	0.035	0.575	0.122	0.680	0.036	0.820	0.0
0.355	0.0	0.510	0.040	0.580	0.120	0.690	0.028	0.830	0.0

TABLE II.- EFFECTIVE ABSORPTION COEFFICIENTS OF WATER VAPOR (cm^2g^{-1})

[From Leckner, 1978*]

λ	k_w	λ	k_w	λ	k_w	λ	k_w	λ	k_w
0.69	0.160E-01	0.84	0.155E+00	0.99	0.125E+00	1.70	0.510E+00	2.90	0.650E+03
0.70	0.240E-01	0.85	0.300E-02	1.00	0.250E-02	1.75	0.400E+01	3.00	0.240E+03
0.71	0.125E-01	0.86	0.100E-04	1.05	0.100E-04	1.80	0.130E+03	3.10	0.230E+03
0.72	0.100E+01	0.87	0.100E-04	1.10	0.320E+01	1.85	0.220E+04	3.20	0.100E+03
0.73	0.870E+00	0.88	0.260E-02	1.15	0.230E+02	1.90	0.140E+04	3.30	0.120E+03
0.74	0.610E-01	0.89	0.630E-01	1.20	0.160E-01	1.95	0.160E+03	3.40	0.195E+02
0.75	0.100E-02	0.90	0.210E+01	1.25	0.180E-03	2.00	0.290E+01	3.50	0.360E+01
0.76	0.100E-04	0.91	0.160E+01	1.30	0.290E+01	2.10	0.220E+00	3.60	0.310E+01
0.77	0.100E-04	0.92	0.125E+01	1.35	0.200E+03	2.20	0.330E+00	3.70	0.250E+01
0.78	0.600E-03	0.93	0.270E+02	1.40	0.110E+04	2.30	0.590E+00	3.80	0.140E+01
0.79	0.175E-01	0.94	0.380E+02	1.45	0.150E+03	2.40	0.203E+02	3.90	0.170E+00
0.80	0.360E-01	0.95	0.410E+02	1.50	0.150E+02	2.50	0.310E+03	4.00	0.450E-02
0.81	0.330E+00	0.96	0.260E+02	1.55	0.170E-02	2.60	0.150E+05		
0.82	0.153E+01	0.97	0.310E+01	1.60	0.100E-04	2.70	0.220E+05		
0.83	0.660E+00	0.98	0.148E+01	1.65	0.100E-01	2.80	0.800E+04		

TABLE III.- TYPICAL ÅNGSTROM TURBIDITY COEFFICIENTS (β_0)

[The original data are converted from Schüepp's turbidity coefficient B through the relation $\beta_0 = 0.935B$. The three decimal digits in the table are a result of this conversion and do not indicate the accuracy; note that $\beta = \beta_0 0.5^{\alpha-1.3}$; from Leckner, 1978*]

Latitude	60°N	45°N	30°N	0°
Low limit	0.01	0.047	0.047	0.047
Medium	0.057	0.077	0.097	0.117
High limit	0.093	0.187	0.375	0.375

*Reprinted with permission from Sol. Energy, vol. 20, copyright 1978, Pergamon Press, Ltd.

TABLE IV.- MEAN OPTICAL DEPTH FOR RAYLEIGH SCATTERING

Zenith angle, deg	Mean optical depth	Zenith angle, deg	Mean optical depth
0	0.094	45	0.088
1		46	.087
2		47	.087
3		48	.087
4		49	.086
5		50	.086
6		51	.086
7		52	.085
8		53	.085
9		54	.084
10		55	.084
11		56	.083
12		57	.083
13		58	.082
14		59	.082
15	.093	60	.081
16		61	.080
17		62	.080
18		63	.079
19		64	.078
20		65	.078
21		66	.077
22		67	.076
23	.092	68	.075
24		69	.074
25		70	.073
26		71	.072
27		72	.071
28		73	.070
29		74	.068
30		75	.067
31	.091	76	.067
32		77	.064
33		78	.062
34		79	.061
35	.090	80	.059
36		81	.056
37		82	.054
38		83	.051
39		84	.048
40	.089	85	.045
41	.089	86	.042
42	.089	87	.037
43	.088	88	.033
44	.088	89	.028

TABLE V.- RELATIVE DECREASE (IN PERCENT) OF THE FLUX OF TOTAL RADIATION FOR THE CASE OF A CONTINUOUS CLOUD COVER OF DIFFERENT TYPES AND DIFFERENT SOLAR ALTITUDES IN COMPARISON WITH THE CORRESPONDING VALUES FOR A CLOUDLESS SKY

[From Kondrat'ev, 1973]

Cloud type	Solar altitude, deg					
	5	10	20	30	40	50
Ci	44	50	34	22	10	2
Cs	33	39	51	35	20	10
Ac	33	39	46	55	46	38
As	44	50	59	64	63	63
St fr.	78	83	80	77	77	76
Sc	89	78	68	71	72	73
St	78	78	80	81	83	84

TABLE VI.- COEFFICIENT a IN EMPIRICAL EQUATION FOR MEAN MONTHLY AND MEAN ANNUAL GLOBAL RADIATION UNDER CLOUDY SKIES

Lat.	0°	5°	10°	15°	20°	25°	30°	35°	40°
a	0.38	0.40	0.40	0.39	0.37	0.35	0.36	0.38	0.38
Lat.	45°	50°	55°	60°	65°	70°	75°	80°	85°
a	0.38	0.40	0.41	0.36	0.25	0.18	0.16	0.15	0.14

TABLE VII.- REGRESSION COEFFICIENTS, THEIR STANDARD ERRORS, AND OTHER STATISTICS FOR HOURLY INSOLATION REGRESSIONS

[From Tarpley, 1979]

	Clear cases ($n < 0.4$)	Partly cloudy ($0.4 \leq n < 1.0$)	Cloudy ($n = 1.0$)
a, ly	-19.33	-9.57	-6.56
b, ly	87.08	94.54	87.68
S_b, ly	0.71	1.78	3.16
c, ly	27.58	-7.62	-7.50
S_c, ly	2.33	0.28	0.35
d, ly	-10.48		
S_d, ly	1.33		
e, ly	-6.37		
S_e, ly	0.79		
Multiple-correlation coefficient	0.94	0.77	0.70
Standard error of the estimate	5.56	12.19	11.36
Number of cases	5736	2127	822

TABLE VIII.- STATISTICS OF ESTIMATED TOTAL DAILY INSOLATION

[From Tarpley, 1979]

	Seven or more pictures per day (dependent data)	Seven or more pictures per day (independent data)	Two pictures per day (dependent data)	One picture per day (dependent data)
Mean error, ly	10.7	17.5	12.4	7.0
Correlation coefficient	0.91	0.90	0.88	0.68
Standard error, ly	50.4	53.5	58.5	99.0
Mean daily insolation (pyranometer), ly	586.2	594.4	586.7	582.8
Number of cases	896	721	1036	1077

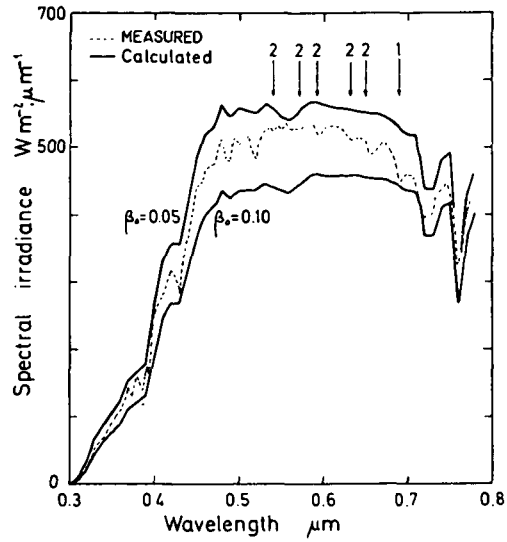

Figure 1.- Calculated direct irradiance on a horizontal surface at air mass 2 and two values of turbidity coefficient β, compared with measured values. The missing weak bands in the calculated curves are indicated with arrows. (From Leckner, 1978; reprinted with permission from Sol. Energy, vol. 20, copyright 1978, Pergamon Press, Ltd.)

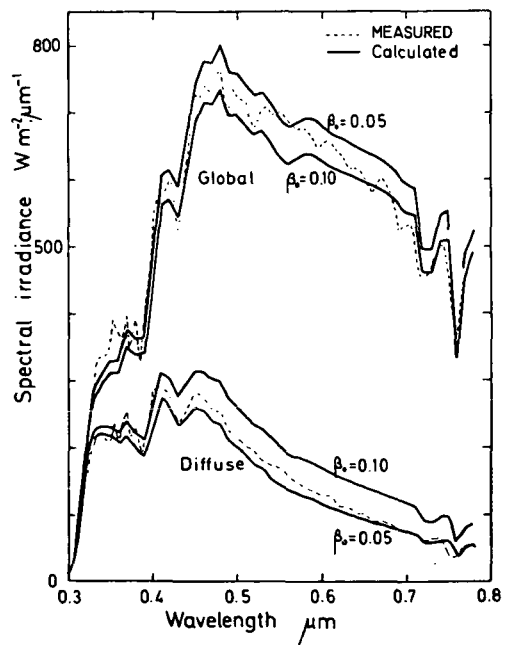

Figure 2.- Calculated global and diffuse irradiances on a horizontal surface at air mass 2 and two values of turbidity coefficient β, compared with measured values. (From Leckner, 1978; reprinted with permission from Sol. Energy, vol. 20, copyright 1978, Pergamon Press, Ltd.)

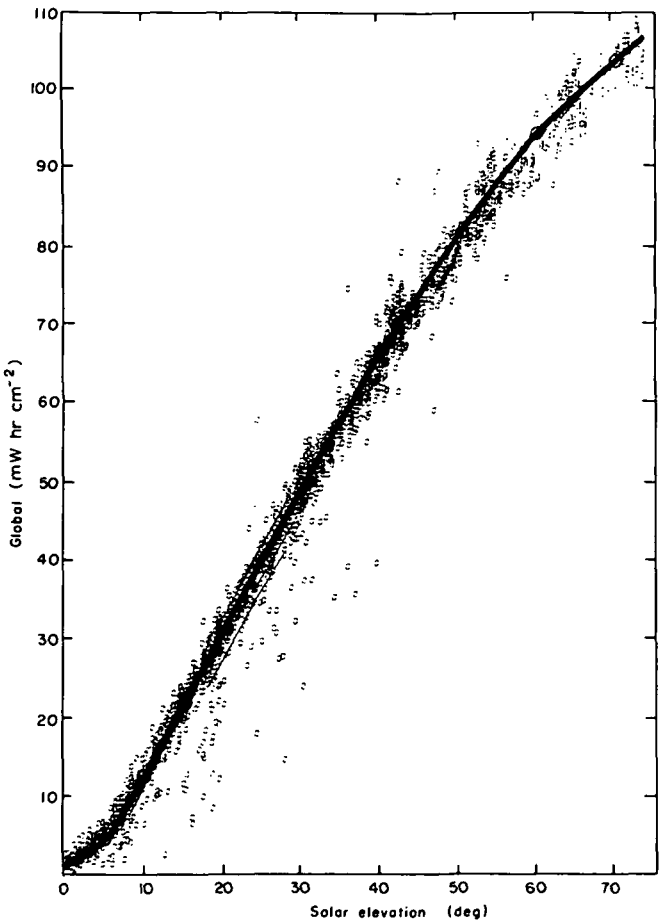

Figure 3.- Global solar radiation (hourly total) in clear skies as a function of solar elevation γ at Aspendale for the period from 1967 to 1972. (From Paltridge and Platt, 1976.)

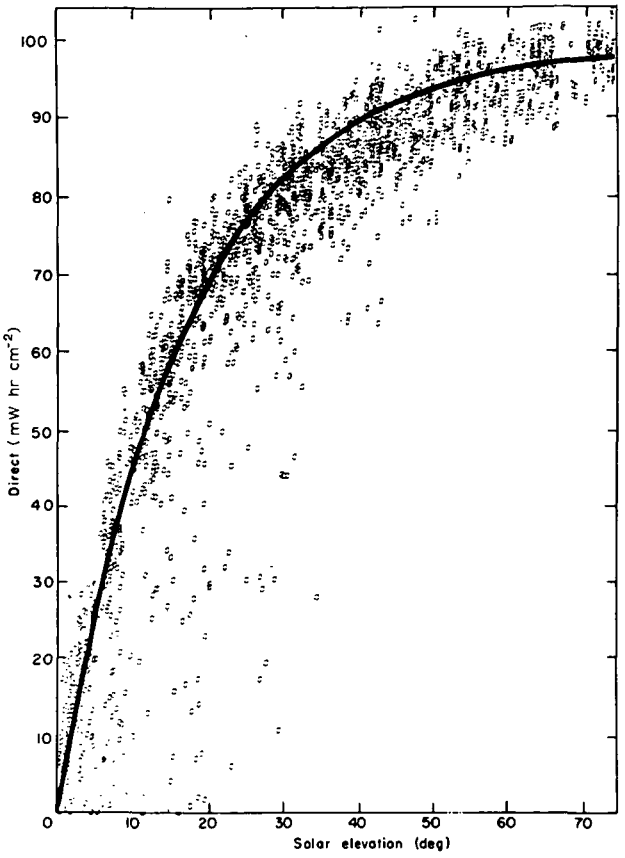

Figure 4.- Direct radiation (hourly total) in clear skies as a function of solar elevation γ at Aspendale for the period from 1967 to 1972. (From Paltridge and Platt, 1976.)

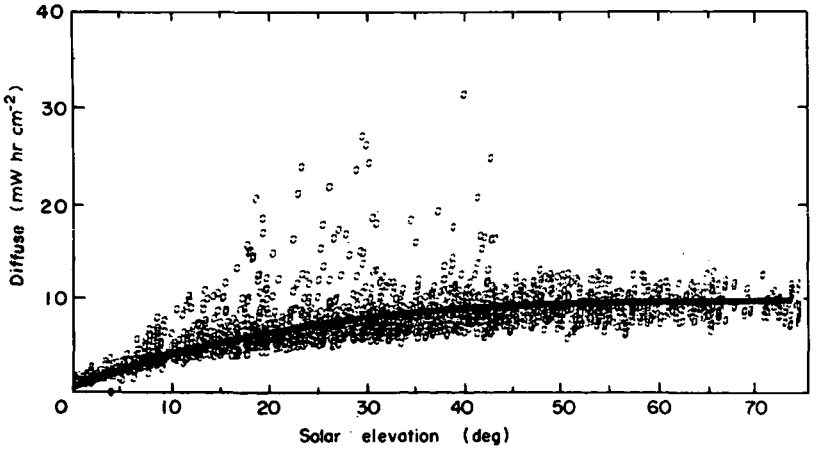

Figure 5.- Diffuse radiation (hourly total) in clear skies as a function of solar elevation angle γ at Aspendale for the period from 1967 to 1972. Note the definition of "clear sky" in the text. (From Paltridge and Platt, 1976.)

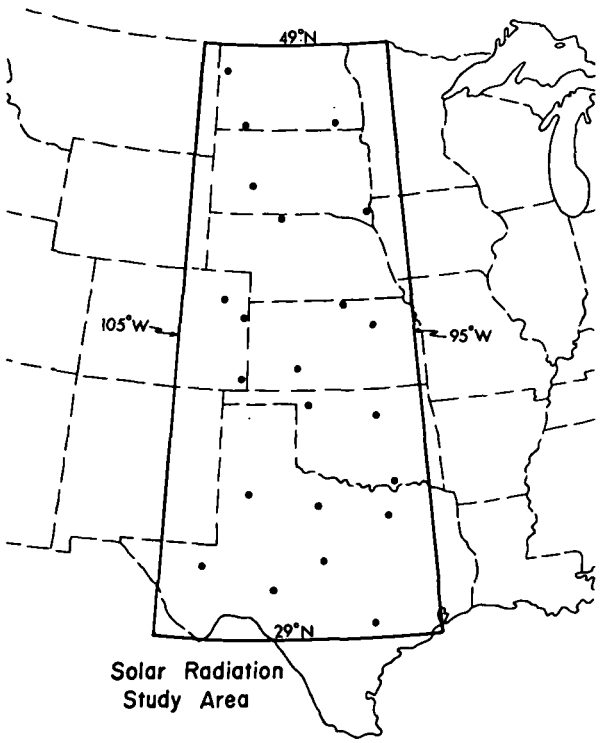

Figure 6.- The part of the Great Plains where satellite data were collected (dark line). The pyranometer sites used in this study are marked with dark circles. (From Tarpley, 1979.)

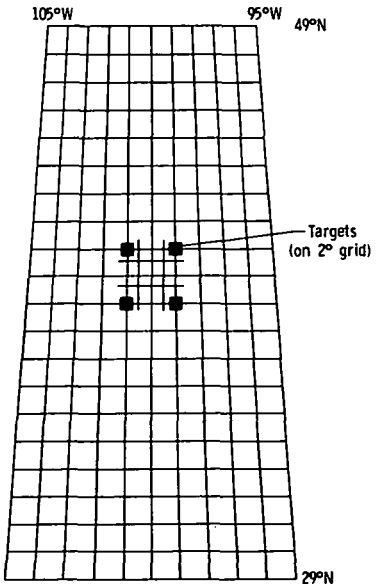

Figure 7.- Grid used for analysis of satellite images.

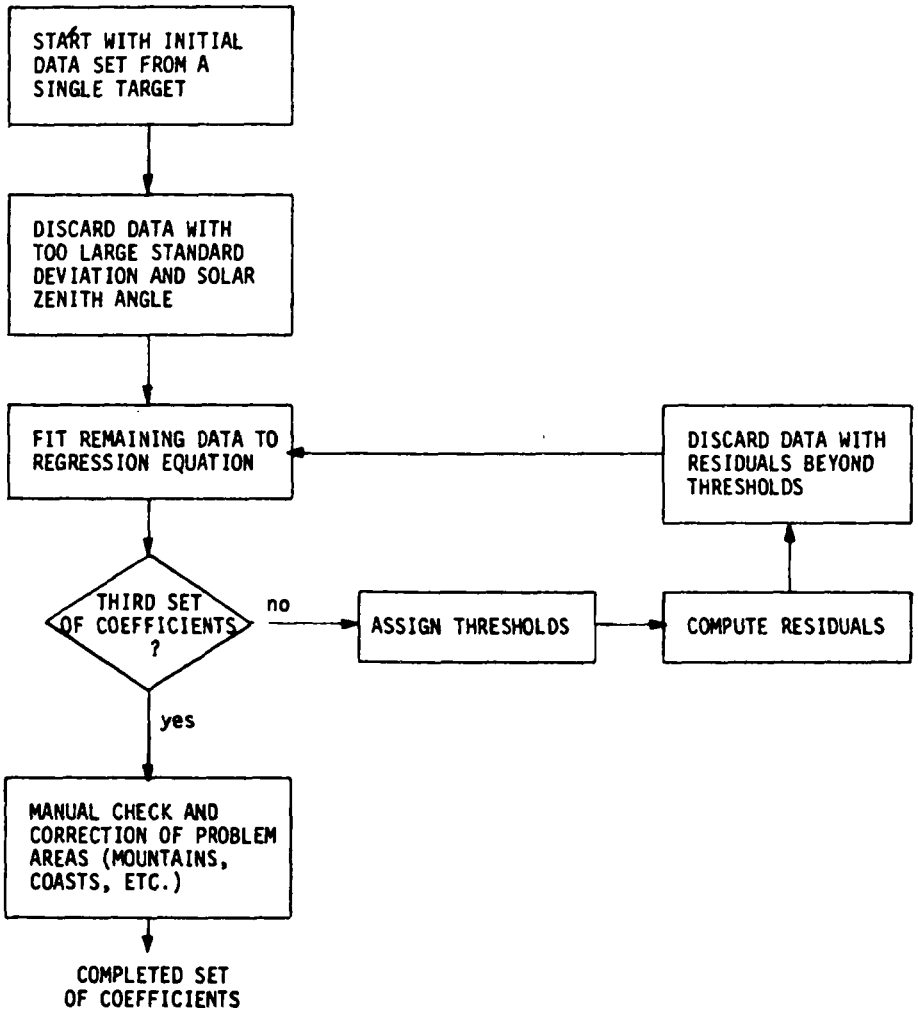

Figure 8.- Flow diagram for processing target brightness data into regression coefficients. (From Tarpley, 1979.)

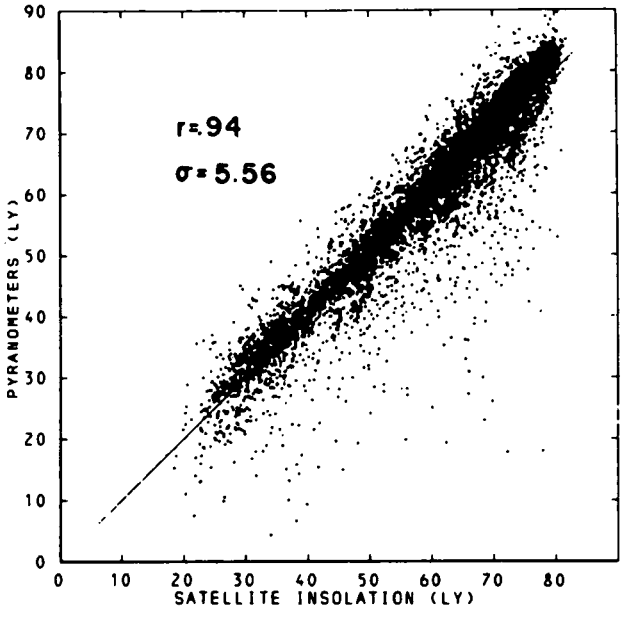

(a) 5736 clear cases ($n < 0.4$).

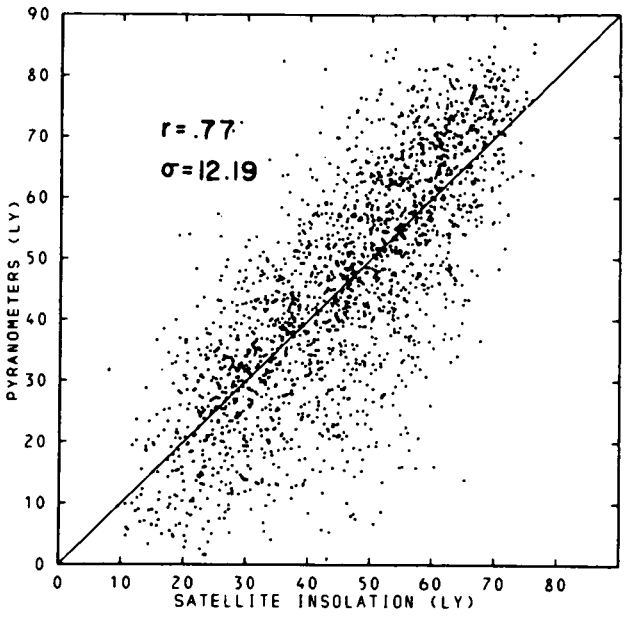

(b) 2217 partly cloudy cases ($0.4 \leq n < 1.0$).

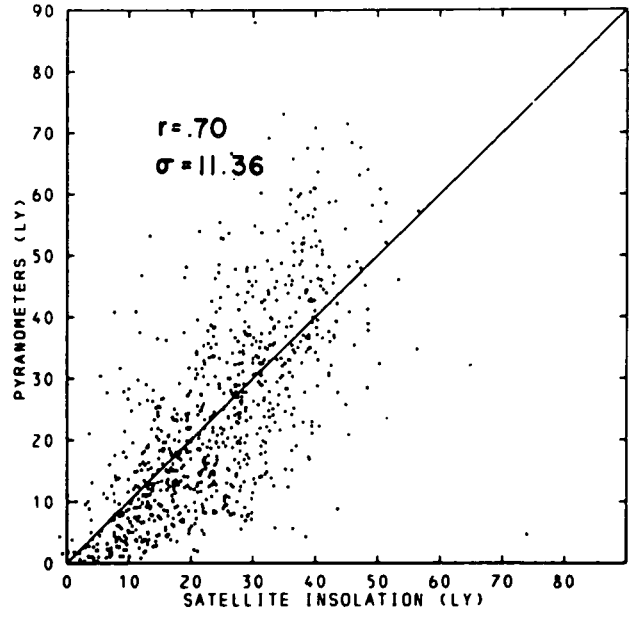

(c) 822 totally cloudy cases ($n = 1.0$).

Figure 9.- Hourly insolation measured by the 22 pyranometers plotted against satellite estimates (dependent data). If there were no errors, all points would lie on the diagonal line. Correlation coefficients r and standard errors σ are shown. (From Tarpley, 1979.)

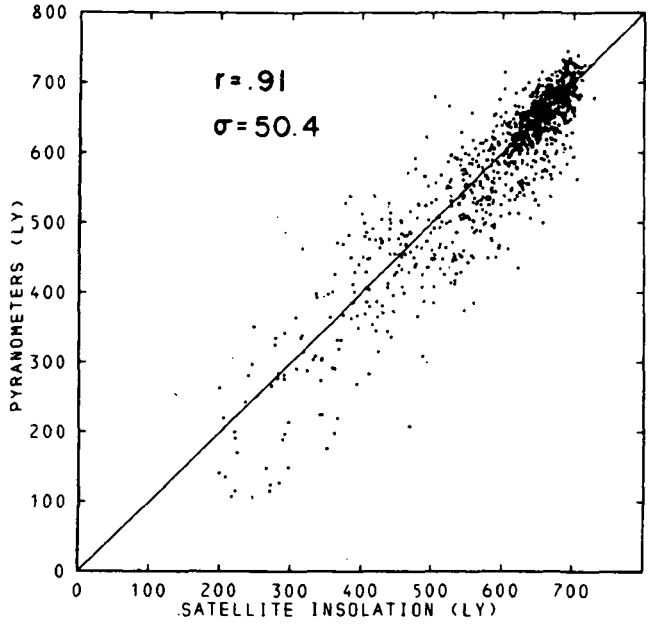

Figure 10.- Daily insolation measured by the 22 pyranometers (dependent data) plotted against satellite estimates (≥7 pictures per day). Diagonal line shows perfect agreement between pyranometers and satellite estimates. (Correlation coefficient r and standard error σ are shown. (From Tarpley, 1979.)